Advances in Concrete Construction, *Vol. 7, No. 3 (2019) 167-174*
DOI: https://doi.org/10.12989/acc.2019.7.3.167

Microstructure modeling of carbonation of metakaolin blended concrete

Xiao-Yong Wang[1a] and Han-Seung Lee[*2]

[1]*Department of Architectural Engineering, Kangwon National University, Chuncheon, Korea*
[2]*Department of Architectural Engineering, Hanyang University, Ansan, Korea*

(Received May 14, 2018, Revised March 3, 2019, Accepted March 13, 2019)

Abstract. Metakaolin (MK), which is increasingly being used to produce high performance concrete, is produced by calcining purified kaolinite between 650 and 700°C in a rotary kiln. The carbonation resistance of metakaolin blended concrete is lower than that of control concrete. Hence, it is critical to consider carbonation durability for rationally using metakaolin in the concrete industry. This study presents microstructure modeling during the carbonation of metakaolin blended concrete. First, based on a blended hydration model, the amount of carbonatable substances and porosity are determined. Second, based on the chemical reactions between carbon dioxide and carbonatable substances, the reduction of concrete porosity due to carbonation is calculated. Furthermore, CO_2 diffusivity is evaluated considering the concrete composition and exposed environment. The carbonation depth of concrete is analyzed using a diffusion-based model. The proposed microstructure model takes into account the influences of concrete composition, concrete curing, and exposure condition on carbonation. The proposed model is useful as a predetermination tool for the evaluation of the carbonation service life of metakaolin blended concrete.

Keywords: metakaolin; carbonation; concrete; model; service life

1. Introduction

Metakaolin (MK) is a reactive aluminosilicate pozzolan and is produced from calcination of the clay mineral kaolinite. Metakaolin is widely used as a supplementary cementitious material to produce high performance concrete. Metakaolin presents many advantages to concrete, such as enhanced workability and finishing ability, increased compressive and flexural strength, and reduced chloride permeability (Badogiannis *et al.* 2002). However, the addition of metakaolin will increase the carbonation depth of concrete. To rationally use metakaolin, the carbonation durability of metakaolin blended concrete should be taken into account (Wang and Lee 2010).

Compared with the abundant experimental results of carbonation of fly ash or slag blended concrete, experimental results about carbonation of metakaolin blended concrete are relatively limited. Meddah *et al.* (2018) found that when metakaolin replaced partial cement, the strength of concrete was improved, but the carbonation resistance was lowered. As the water to binder ratio decreased, carbonation depth of concrete also decreased. Similar with Meddah *et al.*'s (2018) study, Bucher *et al.* (2017) also found the addition of metakaolin increased carbonation depth of concrete. Saillio *et al.* (2015) found that as the curing time before the starting of carbonation increased, the carbonation resistance of metakaolin blended concrete was enhanced. In summary, the carbonation of MK blended concrete relates to water to binder ratio, MK replacement ratio, binder content, and curing of concrete.

On the other hand, some models have been proposed for evaluating carbonation depth of concrete. These models can be classified as the strength-based model, neural network model, statistical model, computational approach, and diffusion-based model. Atis (2004) proposed a strength-based carbonation model for concrete. However, metakaolin presents opposite effects on strength or carbonation. When metakaolin is used to replace partial cement, the strength is enhanced but the carbonation resistance is impaired. In other words, the strength-based carbonation model is generally valid for Portland cement concrete but is not valid for blended concrete. Kwon and Song (2010) made artificial neural networks for analyzing the CO_2 diffusivity and carbonation of concrete. However, the physical meanings of the coefficient matrix of the neural network are not clear because the neural network is a black box predicting technique. Silva *et al.* (2014), Thomas *et al.* (2015) showed statistical modeling of concrete carbonation. Based on the collection of data about carbonation depth, multiple regression was used to find the relation between carbonation and concrete properties and exposure conditions. However, the statistical modeling (Silva *et al.* 2014, Thomas *et al.* 2015) did not consider various processes involved in carbonation, such as the formation of carbonatable substances and concrete porosity, diffusion of CO_2, and chemical reactions between carbonatable substances and CO_2. Saetta and Vitaliani (2004, 2005) took a computational approach to carbonation of concrete. The combination of moisture diffusion, heat transport, CO_2 diffusion, and CO_2 reaction are considered in computational

∗Corresponding author, Professor
E-mail: ercleehs@hanyang.ac.kr
[a]Professor
E-mail: wxbrave@kangwon.ac.kr

ISSN: 2287-5301 (Print), 2287-531X (Online)

approaches. However, computational approaches are mainly focused on carbonation of Portland cement concrete. For MK blended concrete, due to the coexistence of cement hydration and MK reaction, it is difficult to use Saetta and Vitaliani's (2004, 2005) computational approaches. Papadakis (2000), Papadakis and Tsimas (2005), Papadakis *et al.* (2007) proposed a diffusion-based model for analyzing the carbonation of concrete. The amount of carbonatable substances and porosity were calculated using concrete mixtures. However, Papadakis' model assumed the binder fully hydrates regardless of water to binder ratios. In fact, due to the limitation of available capillary water and occupation space, the binder cannot fully hydrate, especially for concrete with low water to binder ratios (Wang and Park 2017). In summary, previous models have various weaknesses, and a new and improved model is necessary for evaluating carbonation of MK blended concrete.

To overcome the weaknesses of previous studies, this study presents a new microstructure model for analyzing the carbonation depth of MK blended concrete. Based on a blended hydration model, the amounts of carbonatable substances and porosity are determined. Furthermore, the CO_2 diffusivity and carbonation depth are evaluated considering concrete compositions and exposed environment. The proposed model is useful as a predetermination tool for evaluating carbonation service life of metakaolin blended concrete.

2. MK blended concrete hydration model

2.1 Hydration model for MK blended concrete

For MK blended concrete, the hydration of cement and the reaction of MK coexist. The hydration of cement can be described using a kinetic model shown in our former studies (Wang and Lee 2010). The degree of hydration α can be calculated as $\alpha = \int_0^t \left(\frac{d\alpha}{dt} \right) dt$ where t is time, and $\frac{d\alpha}{dt}$ is rate of hydration. The kinetic processes involved in cement hydration, such as initial dormant process, phase boundary reaction process, and diffusion process are considered in the cement hydration model. The input parameters of the cement hydration model are cement compound compositions, Blaine surface of cement, concrete mixing proportions, and curing conditions. After inputting these parameters, the reaction degree of cement can be calculated automatically. The effect of curing temperature on cement hydration is considered using the Arrhenius Law. For high strength concrete, the water to cement ratio is low, and the hydration rate is significantly lowered due to the reduction of capillary water. This effect is considered using capillary water concentration. Summarily, the proposed cement hydration model is valid for concrete with different strength levels, different types of Portland cement, and different curing conditions.

MK is a pozzolanic material, and the reaction of MK will consume calcium hydroxide (CH). Considering the producing of CH in cement hydration and the consumption of CH in MK reaction, the CH content in cement-MK blend can be calculated as follows

$$CH(t) = C_0 * RCH_{CE} * \alpha - P * v_{MK} * \alpha_{MK} \quad (1)$$

where $CH(t)$ is calcium hydroxide content, C_0 and P are the mass of cement and MK in concrete mixture, respectively, RCH_{CE} and v_{MK} are the produced CH when 1 unit mass cement hydrates and the consumed CH when 1 unit mass MK reacts, respectively ($v_{MK} = 2.2 - 4.08 * \frac{P}{C_0 + P}$ (Poon *et al* 2001)), and α_{MK} is the reaction degree of MK. $RCH_{CE}*C_0*\alpha$ and $v_{MK}*\alpha_{MK}*P$ are the amount of produced CH content from cement and consumed CH content from MK, respectively.

The amount of chemically combined water W_{cbm} in MK blended concrete is determined as follows

$$W_{cbm} = 0.25 * C_0 * \alpha + 0.24 * P * \alpha_{MK} \quad (2)$$

where 0.25 and 0.24 are the content of chemically combined water when, respectively, 1 unit mass of cement hydrates and 1 unit mass of MK reacts (Murat 1983). Furthermore, $0.25*C_0*\alpha$ and $0.24*P*\alpha_{MK}$ are the contents of chemically combined water produced from hydration reaction of cement and reaction of MK, respectively.

The amount of capillary water W_{cap} in MK blended concrete is calculated as follows

$$W_{cap} = W_0 - 0.4 * C_0 * \alpha - 0.615 * \alpha_{MK} * P \quad (3)$$

where $0.4*C_0*\alpha$ and $0.615*\alpha_{MK}*P$ are the masses of consumed capillary water from cement hydration and MK reaction, respectively (Wang and Lee 2010). The physical bound water of cement hydration products and MK reaction products are $0.15*C_0*\alpha$ and $0.375*\alpha_{MK}*P$, respectively. The physical bound water of 1 unit mass reacted MK is much higher than that of cement. This is because the content of Si in MK is much higher than that in cement. In addition, for cement-MK blends, capillary water concentration C_w can be written as $C_w = \left(\frac{W_{cap}}{W_0} \right)^r$, where r is a factor considering the approachability of capillary water to anhydrous cement (r=1 as water to binder ratio is higher than 0.4, and $r = 2.6 - 4\frac{W_0}{C_0 + P}$ as water to binder ratio is less than 0.4) (Wang and Park 2017).

Kadri *et al.* (2011) made experimental studies on isothermal heat evolution of MK blended cement paste. They found that the reaction process of MK also consisted of an initial dormant process, phase boundary reaction process, and diffusion process, which are similar to the processes involved in the hydration of cement. On the other hand, MK is a pozzolanic material. The reaction rate of a pozzolanic reaction is dependent on the amount of calcium hydroxide in cement-MK blends. Considering the kinetic reaction processes and the essence of MK as a pozzolanic material, the reaction equation of MK is proposed as follows

$$\frac{d\alpha_{MK}}{dt} = \frac{m_{CH}(t)}{P} \frac{3\rho_w}{v_{MK} r_{MK0} \rho_{MK}}$$

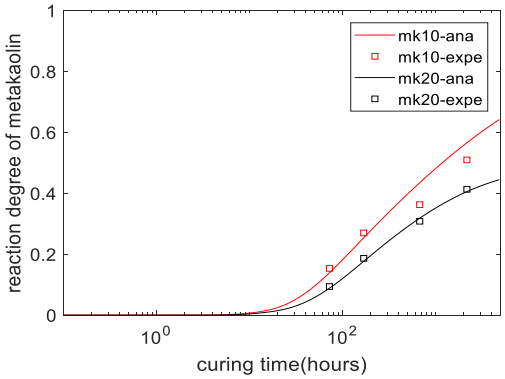

Fig. 1 Reaction degree of metakaolin (MK)

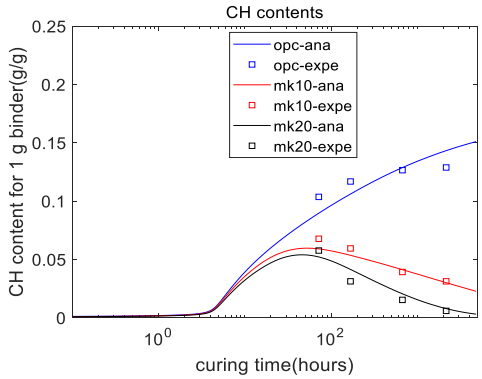

Fig. 2 Calcium hydroxide (CH) content

$$\frac{1}{(\frac{1}{k_{dMK}}-\frac{r_{MK0}}{D_{eMK}})+\frac{r_{MK0}}{D_{eMK}}(1-\alpha_{MK})^{\frac{-1}{3}}+\frac{1}{k_{rMK}}(1-\alpha_{MK})^{\frac{-2}{3}}} \quad (4)$$

$$k_{dMK}=\frac{B_{MK}}{(\alpha_{MK})^{1.5}}+C_{MK}*(\alpha_{MK})^{3} \quad (5)$$

$$D_{eMK}=D_{eMK0}*\ln(\frac{1}{\alpha_{MK}}) \quad (6)$$

where ρ_w is the density of water, r_{MK0} denotes the MK particle radius, ρ_{MK} denotes the MK density, k_{dMK} is the reaction rate parameter in the initial dormant stage (B_{MK} and C_{MK} are reaction parameters of formation of impermeable film and destruction of impermeable film, respectively (Wang and Lee 2010)), D_{eMK0} denotes the initial diffusion coefficient, and k_{rMK} denotes the reaction rate parameter in the phase boundary reaction stage. In Eq. (4), the term $\frac{m_{CH}(t)}{P}$ takes into account the pozzolanic reaction activity of MK.

Summarily, in this section a blended hydration model is proposed to simulate the hydration of cement-MK blends. The kinetic processes involved in the MK reaction, such as initial dormant process, phase boundary reaction process, and diffusion process are considered. The interactions between cement hydration and the MK reaction are considered through the contents of CH and capillary water. The hydration degree of cement and reaction degree of MK are adopted to evaluate the properties of MK blended concrete. In addition, when cement is partially replaced with MK, the water to cement ratio increases. This dilution effect is considered through capillary water concentration C_w.

2.2 Verification of the hydration model

Experimental results in reference (Poon *et al.* 2001) were used to verify the proposed hydration model. Poon *et al.* (2001) measured the reaction degree of MK and CH content for cement-MK paste at the ages of 3 days, 7 days, 28 days, and 90 days. The water to binder ratio was 0.3, the MK replacement ratio was 10% and 20%, and the curing temperature was 20°C. The reaction degree of MK was measured using the selective dissolution method, and the calcium hydroxide content was measured using differential scanning calorimetry.

Based on the reaction degree of MK, the reaction coefficients B_{MK}, C_{MK}, D_{eMK0}, and k_{rMK} were determined as 4.6e-7 cm/h, 0.52 cm/h, 7.21e-7 cm/h, and 3.5e-11 cm^2/h, respectively. The reaction coefficients did not vary with concrete mixtures. The calculated results of reaction degree of MK and calcium hydroxide are shown in Fig. 1 and Fig. 2, respectively.

As shown in Fig. 1, as the MK replacement ratio increased, the activated effect of calcium hydroxide became weaker, and the reaction degree of MK decreased. As shown in Fig. 2, for plain paste without MK, CH content continuously increased as the hydration reaction proceeded. For cement-MK blends, the CH content initially increased because at early ages the production of CH was dominant, while at late ages, the CH content decreased due to the consumption of CH from the MK reaction. In addition, the paste with higher MK content showed lower CH content. For paste with 20% MK, at the age of 90 days, the content of CH was almost zero. Since the proposed blended cement hydration model considers both cement hydration and MK reaction, the proposed model can reflect the general trend of CH evolution of cement-MK blends.

3. Carbonation model

3.1 Evaluation of carbonation depth of MK blended concrete

Papadakis (2000), Papadakis *et al.* (2007) proposed that the carbonatable substances of concrete are calcium hydroxide (CH) and calcium silicate hydrate (CSH). The content of CH can be determined using Eq. (1). The produced CSH from cement hydration and MK reaction can be written as $C_{1.7}SH_4$ and $C_{1.1}SH_{3.9}$, respectively (Wang and Lee 2010). The mass of CSH can be determined as follows (Papadakis 2000, Papadakis *et al.* 2007)

$$CSH_C(t)=3.78*f_{S,C}*C_0*\alpha \quad (7)$$

$$CSH_{MK}(t)=3.19*f_{S,P}*P*\alpha_{MK} \quad (8)$$

where CSH_C and CSH_{MK} are CSH produced from cement hydration and MK reaction, respectively, $f_{S,C}$ and $f_{S,P}$ are

SiO_2 content in cement and MK, respectively. The coefficient 3.78 in Eq. (7) is the mass ratio between molar weight of CSH_C and weight of SiO_2 in CSH_C. The coefficient 3.19 in Eq. (8) is the mass ratio between molar weight of CSH_{MK} and weight of SiO_2 in CSH_{MK}.

The porosity of carbonated concrete can be determined as follows (Papadakis 2000, Papadakis *et al.* 2007)

$$\varepsilon_C = \frac{W_0}{\rho_w} - W_{cbm} - \Delta\varepsilon_C \tag{9}$$

where ε_C is the porosity of carbonated concrete, and $\Delta\varepsilon_C$ is the reduction of porosity due to carbonation of concrete.

For cement-MK blends, the carbonation reactions between CO_2 and carbonatable substances can be described as follows (Maekawa *et al.* 2009, Papadakis 2000, Papadakis *et al.* 2007)

$$Ca(OH)_2 + CO_2 \xrightarrow{K_{CH}} CaCO_3 + H_2O \tag{10}$$

$$1.7CaO \cdot SiO_2 \cdot 4H_2O + 1.7CO_2 \xrightarrow{K_{CSH1}} 1.7CaCO_3 + SiO_2 \cdot 2.5H_2O + 1.5H_2O \tag{11}$$

$$1.1CaO \cdot SiO_2 \cdot 3.9H_2O + 1.1CO_2 \xrightarrow{K_{CSH2}} 1.1CaCO_3 + SiO_2 \cdot 2.5H_2O + 1.4H_2O \tag{12}$$

The density of CSH can be determined as $\rho_{CSH} = 1.71 + 0.249\frac{C}{S}$ where $\frac{C}{S}$ is the Ca/Si ratio in CSH (Tanaka *et al.* 2009). Based on the changing molar volume of solid phases between reactants and products, the reduction of porosity due to concrete carbonation can be determined as

$$\Delta\varepsilon_C = [CH]\Delta V_{CH} + [CSH]_C \Delta V_{CSHC} + [CSH]_{MK} \Delta V_{CSHMK} \tag{13}$$

where ΔV_{CH}, ΔV_{CSHC}, and ΔV_{CSHMK} are changing molar volumes of calcium hydroxide, CSH from hydration of cement, and CSH from reaction of MK, respectively (ΔV_{CH}=3.85*10^{-6} m^3/mol, ΔV_{CSHC}=27.99*10^{-6} m^3/mol, ΔV_{CSHMK}=16.04*10^{-6} m^3/mol).

Carbonation is considerably affected by relative humidity (RH). Carbonation of concrete is commonly greatest when the relative humidity is 50-70%. Once the relative humidity is under 50%, there is insufficient moisture for the carbonation reaction to proceed. For any relative humidity greater than 70%, the diffusion of CO_2 is hindered because of the increase of the saturation amount of concrete pores. For the usual selection of parameters (specifically for relative humidity greater than 55%, CO_2 diffusion controlled carbonation process (Papadakis 2000)), a carbonation front will occur, which distinguishes concrete into two parts: a complete carbonation part, and a part by which concrete carbonation has not begun whatsoever. The space between this carbonation front and the outer concrete surface is known as carbonation depth. For the most typical one-dimensional cases, its evolution as time passes is offered with a simple analytical expression, with regards to the composition as well as the exposure conditions. The evolution of concrete carbonation depth x_c (m) with time t (s), is calculated as follows (Papadakis 2000)

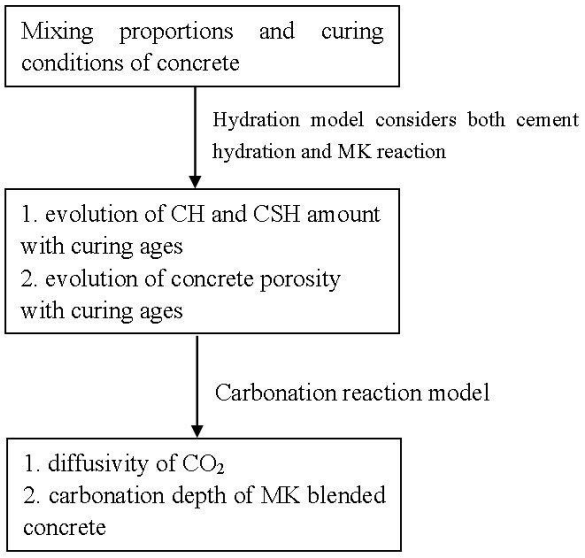

Fig. 3 The flowchart of integrated hydration–carbonation model

$$x_c = \sqrt{\frac{2D_C[CO_2]_0 t}{[\mathrm{CH}] + 1.7[\mathrm{CSH}]_C + 1.1[\mathrm{CSH}]_{MK}}} \tag{14}$$

$$D_C = A\left(\frac{\varepsilon_C}{\frac{C_0}{\rho_c} + \frac{P}{\rho_{MK}} + \frac{W_0}{\rho_w}}\right)^a \left(1 - \frac{RH}{100}\right)^{2.2} \tag{15}$$

where D_C is the CO_2 diffusivity, $[CO_2]_0$ is the concentration of CO_2, ρ_c is density of cement, ρ_w is density of water, RH is relative humidity of the exposure environment, and A and a are carbonation parameters of concrete. The carbonation parameters A and a do not vary with concrete mixtures.

The summary of integrated hydration-carbonation model is shown in Fig. 3. After inputting the concrete mixtures and curing conditions, the development of concrete properties, such as the contents of CH, CSH, and porosity, can be calculated as evolutions of curing ages. The calculation results from the hydration model are used as input parameters for carbonation model. Based on the diffusion-based carbonation model, the carbonation depth of concrete can be determined. In addition, because the carbonation happens in the surface zone of concrete, the relative humidity in the carbonation zone is assumed to be same as RH in the surrounding environment.

3.2 Verification of the carbonation model

The experimental results in reference (Meddah *et al.* 2018) were used to verify the proposed carbonation model. Meddah *et al.* (2018) measured carbonation depth of concrete with different MK replacement ratios (from 5% to 20%) and different water to binder ratios (0.52 and 0.65). The mixing proportions of concrete are shown in Table 1. The acceleration carbonation tests started after 28 days curing. The size of the cubic carbonation specimen was 100

Table 1 Concrete mixing proportions

	Water (kg/m^3)	Cement (kg/m^3)	Metakaolin (kg/m^3)	Sand (kg/m^3)	Coarse aggregate (kg/m^3)
WB65-mk0	185	285	-	730	1200
WB65-mk5	185	270.75	14.25	730	1200
WB65-mk10	185	256.5	28.5	730	1200
WB65-mk15	185	242.25	42.75	730	1200
WB65-mk20	185	228	57	730	1200
WB52-mk0	185	355	-	670	1200
WB52-mk5	185	337.25	17.75	670	1200
WB52-mk10	185	319.5	35.5	670	1200
WB52-mk15	185	301.75	53.25	670	1200
WB52-mk20	185	284	71	670	1200

mm. Five faces of the specimen were sealed and one surface was exposed to CO_2 in a carbonation chamber. The CO_2 concentration in the carbonation chamber was 4%, the temperature was 20℃, and the relative humidity was 55%. The carbonation depth was measured using phenolphthalein indicator after 20 weeks of exposure.

The development of properties of MK blended concrete is shown in Fig. 4. As shown in Fig. 4(a), the addition of MK enhanced the degree of cement hydration. This was because of the dilution effect of MK. Moreover, as water to binder increased, the reaction degree of cement also increased. This was because of the increasing capillary water concentration.

As shown in Fig. 4(b), as the replacement ratio of MK

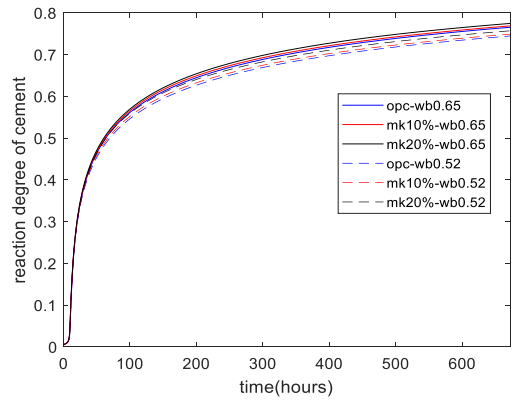

(a) Reaction degree of cement

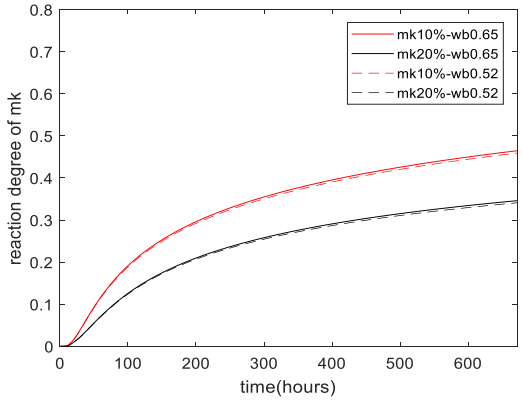

(b) Reaction degree of MK

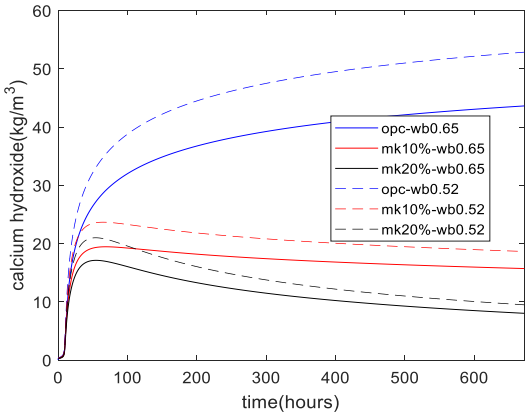

(c) Calcium hydroxide content

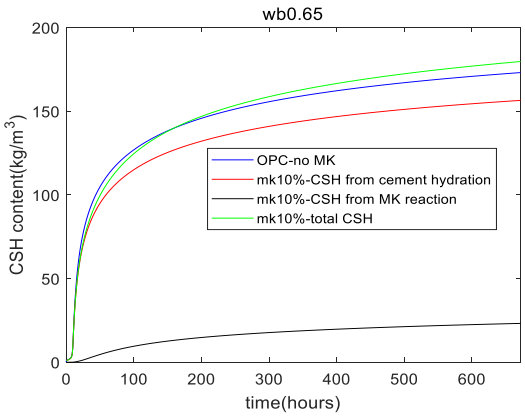

(d) CSH content

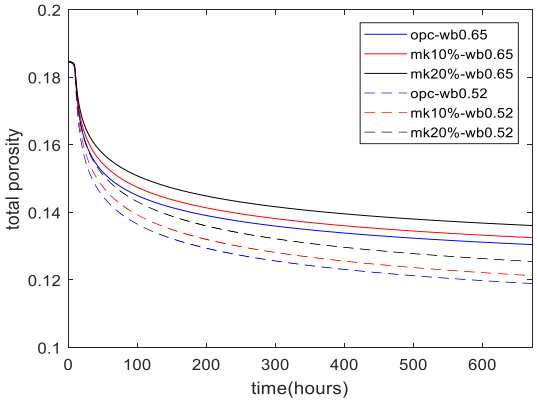

(e) Porosity of hardening concrete

Fig. 4 Properties development of MK blended concrete

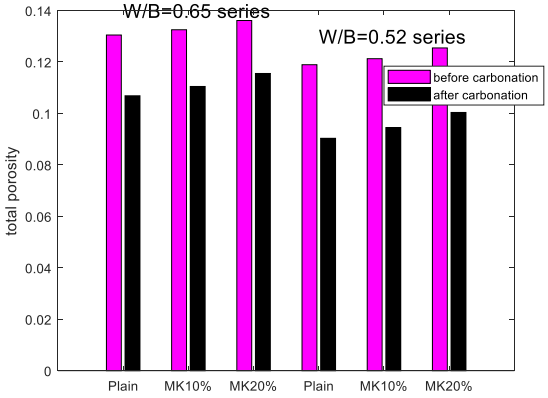

(a) Porosity reduction

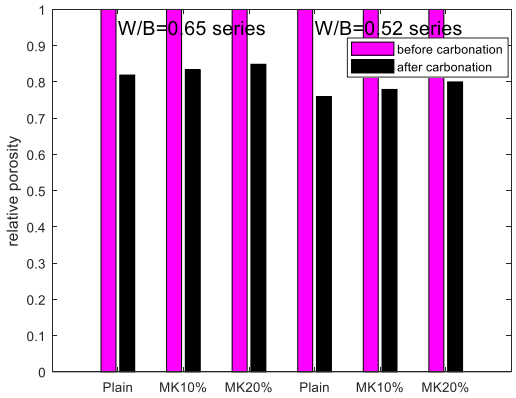

(b) Relative porosity after carbonation

Fig. 5 Porosity reduction due to carbonation

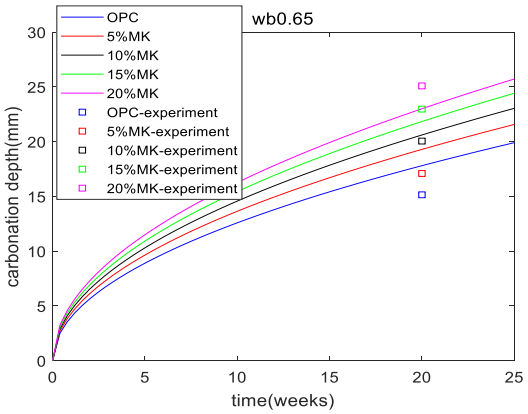

(a) Water to binder ratio 0.65

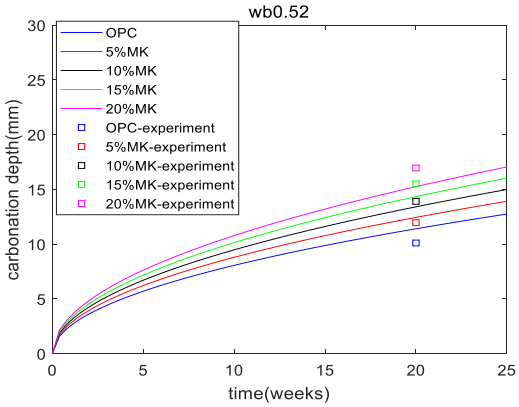

(b) Water to binder ratio 0.52

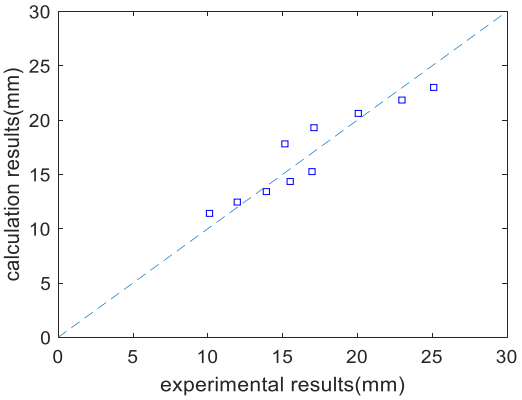

(c) Comparison between calculation results and experiment results

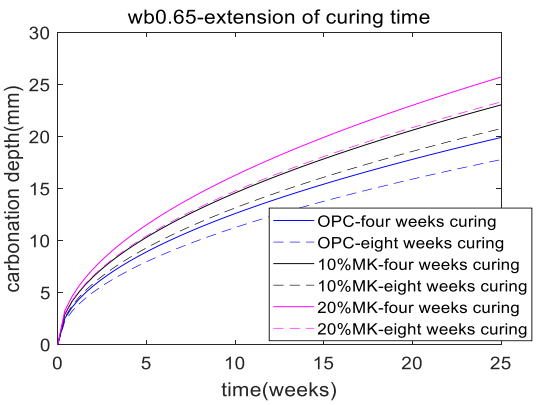

(d) Effect of curing time on carbonation

Fig. 6 Analysis of carbonation depth

increased, the reaction degree of MK decreased due to the reduction of the alkali activation effect of calcium hydroxide. In addition, as the water to binder ratio changed from 0.52 to 0.65, the increase of the reaction degree of MK was not obvious.

Fig. 4(c) shows the calcium hydroxide content. As the water to binder ratio changed from 0.52 to 0.65, calcium hydroxide content decreased because of the reduction of binder content. The concrete with a higher water to binder ratio of 0.65 and a higher MK replacement ratio of 20% had the lowest calcium hydroxide content.

Fig. 4(d) shows CSH content for control concrete and MK 10% concrete with a water to binder ratio of 0.65. At early ages, due to the dilution effect, the CSH content of MK blended concrete was slightly lower than that of control concrete, while at late ages, due to the proceeding of the MK reaction, CSH content of MK blended concrete was higher than that of control concrete.

Fig. 4(e) shows the porosity of hardening concrete. As the water to binder ratio increased, porosity of concrete increased. The addition of MK increased the total porosity of concrete. Frias and Cabrera (2000), Khatib and Wild

(1996) also found that MK blended concrete had higher total porosity than control concrete. This is because the reactivity of MK is slower than cement. On the other hand, although the total porosity of MK blended concrete was higher, the content of finer pores in MK blended concrete was higher than control concrete due to the pore size refinement and grain size refinement of MK (Kannan 2018, Singh and Siddique 2017, Papadakis 1999).

In Meddah *et al*'s studies (2018), the relative humidity in the CO_2 chamber was 55%. The hydration of the binder hardly proceeded when the relative humidity was less than 80% (Wang and Lee 2010). Hence further hydration of the binder in the carbonation zone during carbonation was not considered in this study. Based on Eq. (9) and Eq. (13), the porosity reduction after carbonation was calculated and is shown in Fig. 5(a). Relative porosity refers to the ratio of porosity after carbonation to the porosity before carbonation. As shown in Fig. 5(b), as the water to binder ratio decreased, the reduction of porosity due to carbonation became obvious. This was because the concrete with a lower water to binder ratio had higher binder content and a higher content of carbonatable substances. Houst and Wittmann (1994) also found similar experimental results about porosity reduction for carbonated concrete. Moreover, as the MK replacement ratio increased, the reduction of porosity due to carbonation became indiscernible. This may be due to the reduction of calcium hydroxide content and the changing of molar volume for different CSH. Ngala and Page (1997) also found similar results. For fly ash or slag blended concrete, the porosity reduction due to carbonation was less than plain concrete (Ngala and Page 1997).

The calculation results from the hydration model, such as CH content, CSH content, and concrete porosity, were used as input parameters for the carbonation model. Furthermore, based on experimental results about carbonation depths of metakaolin blended concrete with different MK content and different water to binder ratios, the carbonation parameters of Eq. (15) could be determined as A=1.29e-6, a=2.84. The values of carbonation parameters did not vary with concrete mixtures. The values of carbonation parameters general agreed with those in other studies (Papadakis 2000, Papadakis *et al*. 2007). The calculation results of carbonation depth are shown in Fig. 6. Fig. 6(a) and Fig. 6(b) show that the addition of MK in concrete increased the carbonation depth of concrete. As the water to binder ratio changed from 0.65 to 0.52 (from Fig. 6(a) to Fig. 6(b)), the carbonation depth of concrete decreased. Fig. 6(c) shows the analysis results generally agreed with experimental results. The correlation coefficient between analysis results and experimental results was 0.94. Fig. 6(d) shows the effect of pre-curing time on carbonation depth of concrete. As the curing time before carbonation tests increased from four to eight weeks, the carbonation depth of concrete decreased. Summarily, based on the analysis results about concrete carbonation, a lower water to binder ratio and a longer pre-curing period before carbonation can be used to increase the carbonation resistance of concrete.

4. Conclusions

This study presents an integrated modeling about hydration and carbonation of metakaolin blended concrete.

First, a blended cement hydration model is proposed to simulate the hydration of cement-MK blends. The kinetic hydration model of MK considers the processes involved in the MK reaction and the dependence of the MK reaction on calcium hydroxide. The coefficients of the hydration model do not vary with concrete mixtures. Based on the blended hydration model, the amounts of carbonatable substances and porosity are determined.

Second, based on the reactions between carbon dioxide and carbonatable substances, the reduction of porosity due to carbonation is calculated. As the water to binder decreases, the reduction of porosity due to carbonation becomes significant. As the MK replacement ratio increases, the reduction of porosity due to carbonation becomes not obvious.

Furthermore, the CO_2 diffusivity and carbonation depth are evaluated considering concrete composition and exposed environment. The proposed microstructure model considers concrete composition, concrete curing, and exposure condition on carbonation, and is useful as a predetermination tool for evaluation of carbonation service life of metakaolin blended concrete.

Acknowledgments

This research was supported by the Basic Science Research Program through the National Research Foundation of Korea (NRF), funded by the Ministry of Science, ICT and Future Planning (No. 2015R1A5A1037548), and an NRF grant (NRF-2017R1C1B1010076).

Reference:

Atis, C.D. (2004), "Carbonation-porosity-strength model for fly ash concrete", *J. Mater. Civil Eng.*, **16**(1), 91-94.

Badogiannis, E., Tsivilis, S., Papadakis, V. and Chaniotakis, E. (2002), "The effect of metakaolin on concrete properties", *International Congress: Challenges of Concrete Construction. In Innovations and Developments in Concrete Materials and Construction,* Eds. R.K. Dhir, P.C. Hewlett, and L.J. Cetenyi, Dundee, Scotland.

Bucher, R., Diederich, P., Escadeillas, G. and Cyr, M. (2017), "Service life of metakaolin-based concrete exposed to carbonation comparison with blended cement containing fly ash, blast furnace slag and limestone filler", *Cement Concrete Res.*, **99**, 18-29.

Frias, M. and Cabrera, J. (2000), "Pore size distribution and degree of hydration of metakaolin-cement pastes", *Cement Concrete Res.*, **30**(4), 561-569.

Houst, Y.F. and Wittmann, F.H. (1994), "Influence of porosity and water content on the diffusivity of CO_2 and O_2 through hydrated cement paste", *Cement Concrete Res.*, **24**(6), 1165-1176.

Kadri, E. H., Kenai, S., Ezziane, K., Siddique, R. and De Schutter, G. (2011), "Influence of metakaolin and silica fume on the heat of hydration and compressive strength development of mortar", *Appl. Clay Sci.*, **53**(4), 704-708.

Kannan, V. (2018), "Strength and durability performance of self compacting concrete containing self-combusted rice husk ash and metakaolin", *Constr. Build. Mater.*, **160**, 169-179.
Khatib, J.M. and Wild, S. (1996), "Pore size distribution of metakaolin paste", *Cement Concrete Res.*, **26**(10), 1545-1553.
Kwon, S.J. and Song, H.W. (2010), "Analysis of carbonation behaviour in concrete using neural network algorithm and carbonation modelling", *Cement Concrete Res.*, **40**(1), 119-127.
Maekawa, K., Ishida, T. and Kishi, T. (2009), *Multi-scale Modeling of Structural Concrete*, Taylor & Francis, London and New York.
Meddah, M.S., Ismail, M.A., El-Gamal, S. and Fitriani, H. (2018), "Performances evaluation of binary concrete designed with silica fume and metakaolin", *Constr. Build. Mater.*, **166**, 400-412.
Murat, M. (1983), "Hydration reaction and hardening of calcined clays and related materials I. preliminary investigation on meta kaolinite", *Cement Concrete Res.*, **13**(2), 259-266.
Ngala, V.T. and Page, C.L. (1997), "Effects of carbonation on pore structure and Diffusional properties of hydrated cement pastes", *Cement Concrete Res.*, **27**(7), 995-1007.
Papadakis, V.G. (1999), "Experimental investigation and theoretical modeling of silica fume activity in concrete", *Cement Concrete Res.*, **29**(1), 79-86.
Papadakis, V.G. (2000), "Effect of supplementary cementing materials on concrete resistance against carbonation and chloride ingress", *Cement Concrete Res.*, **30**(2), 291-299.
Papadakis, V.G. and Tsimas, S. (2005), "Greek supplementary cementing materials and their incorporation in concrete", *Cement Concrete Compos.*, **27**(2), 223-230.
Papadakis, V.G., Efstathiou, M.P. and Apostolopoulos, C.A. (2007), "Computer-aided approach of parameters influencing concrete service life and field validation", *Comput. Concrete*, **4**(1), 1-18.
Poon, C.S., Lam, L., Kou, S.C., Wong, Y.L. and Wong, R. (2001), "Rate of pozzolanic reaction of metakaolin in high-performance cement pastes", *Cement Concrete Res.*, **31**(9), 1301-1306.
Saetta, A.V. and Vitaliani, R.V. (2004), "Experimental investigation and numerical modeling of carbonation process in reinforced concrete structures Part I: theoretical formulation", *Cement Concrete Res.*, **34**(4), 571-579.
Saetta, A.V. and Vitaliani, R.V. (2005), "Experimental investigation and numerical modeling of carbonation process in reinforced concrete structures, part II: practical applications", *Cement Concrete Res.*, **35**(5), 958-967.
Saillio, M., Baroghel-Bouny, V. and Pradelle, S. (2015), "Various durability aspects of calcined Kaolin-Blended portland cement pastes and concretes", Eds. K. Scrivener and A. Favier, *Proceedings of 1st International Conference on Calcined Clays for Sustainable Concrete*, 491-499.
Silva, A., Neves, R. and de Brito, J. (2014), "Statistical modelling of carbonation in reinforced concrete", *Cement Concrete Compos.*, **50**, 73-81.
Singh, G.A. and Siddique, R. (2017), "Strength and micro-structural properties of self-compacting concrete containing metakaolin and rice husk ash", *Constr. Build. Mater.*, **157**, 51-64.
Tanaka, Y., Saeki, T., Sasaki, K. and Suda, Y. (2009). "Fundamental study on density of c-s-h", *Cement Sci. Concrete Technol.*, **63**(1), 70-76.
Thomas, P.H., Fabiana, G., Nicholas, H.F. and Paul, S.F. (2015), "Statistical analysis of the carbonation rate of concrete", *Cement Concrete Res.*, **72**, 98-107.
Wang, X.Y. and Lee, H.S. (2010), "Modeling the hydration of concrete incorporating fly ash or slag", *Cement Concrete Res.*, **40**(7), 984-996.
Wang, X.Y. and Park, K.B. (2017), "Analysis of the compressive strength development of concrete considering the interactions between hydration and drying", *Cement Concrete Res.*, **102**, 1-15.

JK